BMC Microbiology

RESEARCH Open Access

Synthesis and characterization of TiO_2 nanoparticles combined with geraniol and their synergistic antibacterial activity

Almotasem Bellah Younis[1], Vedran Milosavljevic[1], Tatiana Fialova[1], Kristyna Smerkova[1], Hana Michalkova[1], Pavel Svec[1], Peter Antal[2], Pavel Kopel[2], Vojtech Adam[1], Ludek Zurek[1] and Kristyna Dolezelikova[1*]

Abstract

Background The emergence of antibiotic resistance in pathogenic bacteria has become a global threat, encouraging the adoption of efficient and effective alternatives to conventional antibiotics and promoting their use as replacements. Titanium dioxide nanoparticles (TiO_2 NPs) have been reported to exhibit antibacterial properties. In this study, we synthesized and characterized TiO_2 NPs in anatase and rutile forms with surface modification by geraniol (GER).

Results The crystallinity and morphology of modified TiO_2 NPs were analyzed by UV/Vis spectrophotometry, X-ray powder diffraction (XRD), and scanning electron microscopy (SEM) with elemental mapping (EDS). The antimicrobial activity of TiO_2 NPs with geraniol was assessed against *Staphylococcus aureus*, methicillin-resistant *Staphylococcus aureus* (MRSA), and *Escherichia coli*. The minimum inhibitory concentration (MIC) values of modified NPs ranged from 0.25 to 1.0 mg/ml against all bacterial strains, and the live dead assay and fractional inhibitory concentration (FIC) supported the antibacterial properties of TiO_2 NPs with GER. Moreover, TiO_2 NPs with GER also showed a significant decrease in the biofilm thickness of MRSA.

Conclusions Our results suggest that TiO_2 NPs with GER offer a promising alternative to antibiotics, particularly for controlling antibiotic-resistant strains. The surface modification of TiO_2 NPs by geraniol resulted in enhanced antibacterial properties against multiple bacterial strains, including antibiotic-resistant MRSA. The potential applications of modified TiO_2 NPs in the biomedical and environmental fields warrant further investigation.

Keywords Titanium dioxide, Nanoparticles, Geraniol, Minimum inhibitory concentration, Biofilm, Methicillin-resistant *Staphylococcus aureus*, MRSA, *Escherichia coli*, SEM-EDS

*Correspondence:
Kristyna Dolezelikova
kriki.cihalova@seznam.cz
[1]Department of Chemistry and Biochemistry, Mendel University in Brno, Brno, Czech Republic
[2]Department of Inorganic Chemistry, Faculty of Science, Palacky University, Olomouc, Czech Republic

Background

Spread of antibiotic-resistant bacteria is a major concern worldwide due to infections leading to high morbidity and mortality rates [1, 2]. The impact of antibiotic resistance on health and disease has been further underlined by recent developments in understanding the microbiome [3–5].To combat this issue, alternative compounds such as natural products and nanoparticles have been explored [6]. Metallic nanoparticles (NPs) such as zinc, cerium, aluminum, nickel, zirconium, magnesium, and titanium dioxide have the potential to act as antimicrobial agents due to their small size and high surface-to-volume ratio [7–11]. In particular, titanium dioxide has been shown to have enhanced photoelectrochemical performance and effective photocatalytic properties [12, 13] These properties allow them to generate reactive oxygen species (ROS), such as hydrogen peroxide, hydroxyl radicals, and superoxide anions, that can penetrate bacterial cell walls and disrupt cell functions, leading to cell death [14–16]. Additionally, NPs can be modified with organic compounds to enhance their antimicrobial activity, making them promising candidates for treating infections caused by antibiotic-resistant bacterial strains [17, 18]. One of the NPs that has gained attention for its antimicrobial properties is titanium dioxide (TiO_2) [14].

Titanium dioxide (TiO_2) is a unique material that displays various physical and chemical characteristics, including the ability to produce ROS when exposed to light, creating pairs of holes. These electron-hole pairs can react with water or oxygen and, as a result, generate ROS [19, 20] Multiple studies have demonstrated that TiO_2 exhibits good antibacterial and antifungal activity against a broad range of Gram-positive and Gram-negative bacteria [21]. TiO_2 has three different crystalline phases: rutile, anatase, and brookite; each can exhibit metastable behavior as various factors affect its crystal shape and cause a possible conversion among the three phases [22, 23]. It was shown that anatase and rutile phases are stable and have great photocatalytic activity [24–26]. The cytotoxicity of TiO_2 varies depending on the crystal shape, as results of several studies showed that the toxicity of TiO_2 was dependent on the concentration and the crystal phase; therefore, the response of bacteria to the crystals can be different [16, 27–29].

Using natural compounds can greatly enhance the inherent physical and chemical properties of NPs [30, 31]. For instance, TiO_2 has been used as an antimicrobial additive in polyamide 12 powder, and nitrogen-doped titanium dioxide nanoparticles have demonstrated photoinduced antimicrobial properties under visible-light irradiation [32, 33] The small size, high surface energy, and strong hydrophilicity for surface hydroxylation may increase TiO_2 NPs compatibility with polymer materials [34, 35]. Incorporating inorganic NPs into organic polymeric nanocomposites is a promising strategy to enhance their antimicrobial properties [36–38]. For example, monoterpenes incorporated with TiO_2 had a greater antimicrobial effect [39]. Monoterpenes are natural products containing active compounds such as phenols, flavonoids, and terpenoids. Geraniol is a monoterpenoid with low toxicity and high solubility, and when combined with TiO_2 NPs, it may exhibit enhanced antimicrobial properties [40, 41].

The objectives of this study were to: (a) synthesize TiO_2 NPs and combine them with geraniol; (b) assess the antimicrobial activity of this material against planktonic and biofilm-forming bacterial cells. This is a novel study focusing on the combined effect of geraniol and TiO_2 NPs and their synergistic activity against *E. coli, Staphylococcus aureus*, and MRSA. This distinguishes it from the previous studies that have mainly focused on the effects of individual agents.

Results

Characterization of the TiO_2 NPs

Synthesized TiO_2 NPs and their combination with GER were characterized through elemental analysis, and GER was detected on the surface of TiO_2. Scanning electron microscopy revealed the size, shape, and surface morphology of the anatase and rutile TiO_2 material and showed that NPs were successfully formed. The anatase form of the TiO_2 had clusters of particles with an average size of 300 ± 100 nm. High-magnification imaging revealed dense nanocrystalline domains on the surface. The anatase form of the TiO_2 with GER resembled unmodified TiO_2 NPs, did not vary in size after surface modification with GER, and showed a strong tendency for aggregate. However, imaging revealed nanocrystalline domains and a relatively smooth surface (Fig. 1A, B), compared to the unmodified form of TiO_2 indicating the presence of GER on the surface. In the rutile form of TiO_2 without surface modification (Fig. 1A, B), the nanoparticles (NPs) had irregular rock shapes with an average size of 100 ± 10 nm and a tendency to aggregate. The same properties were observed for the rutile form of the TiO_2 NPs modified with GER. However, in the case of the rutile form, the surface was not smooth as it did in the case of the anatase form after modification with GER. To further confirm the presence of GER on the surface of TiO_2 NPs, we used the energy-dispersive X-ray spectroscopy (EDS) for an elemental mapping analysis. The elemental dispersion on the TiO_2 surface in both forms showed the presence of carbon, which confirms the successful modification with GER. Both non-modified forms also showed signs of carbon; however, in trace amounts (contamination for ambiance) only (Fig. 1).

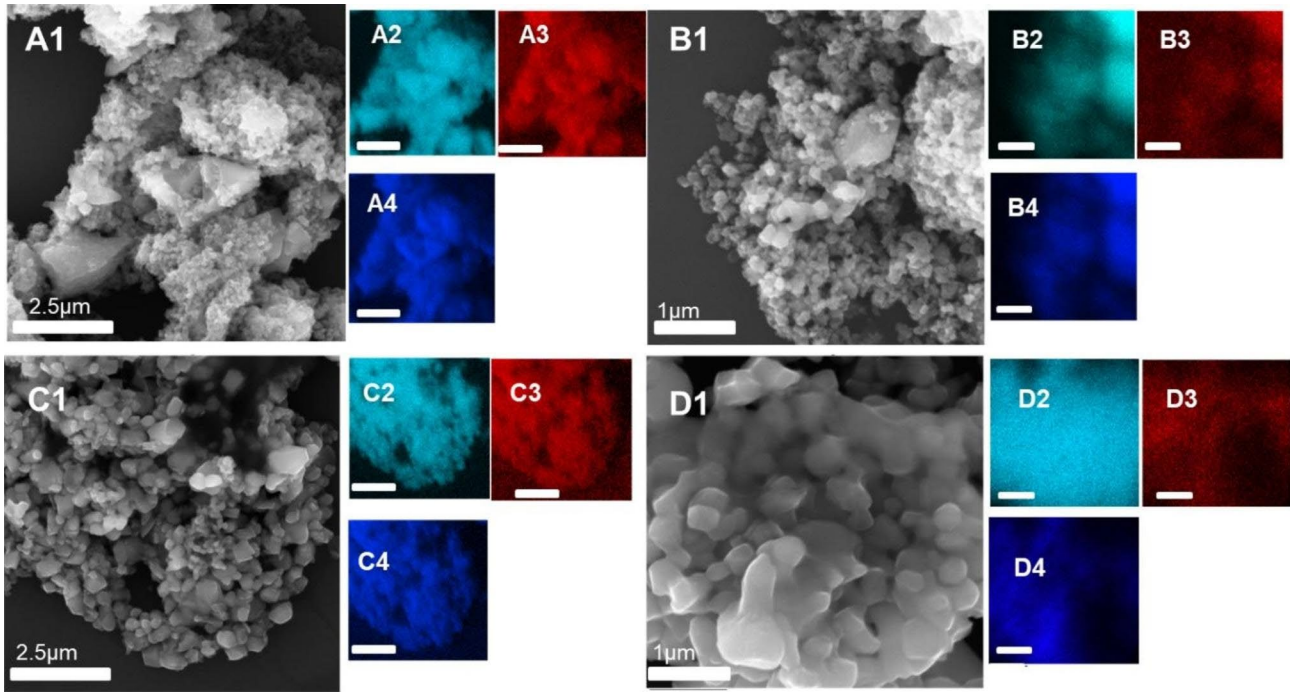

Fig. 1 SEM images of unmodified and modified TiO_2 NPs. A1-A4 unmodified anatase TiO_2 NPs and their corresponding surface elements (Ti, C, and O, respectively). B1-B4 unmodified rutile TiO_2 NPs and their corresponding surface elements (Ti, C, and O, respectively). C1-C4 and D1-D4. Modified anatase and rutile TiO_2 NPs and their corresponding surface elements (Ti, C, and O, respectively).

X-ray crystallography (XRD) patterns confirmed the crystallinity of the TiO_2 (anatase and rutile) observed under SEM. These patterns showed that both forms of TiO_2 NPs were polycrystalline with well-defined peaks indicating a high degree of crystallinity. The XRD pattern exhibited diffraction peaks at 27.26°, 36.14°, 41.16°, 43.79°, 54.23°, 56.30°, 62.92°, and 68.67°, which belongs to the anatase and tetragonal rutile form of TiO_2 NPs [42, 43] (Fig. 2). These results indicate that increasing the temperature without using any additive changed the biphasic anatase/rutile to rutile TiO_2 NPs.

To confirm the presence of GER on the surface of TiO_2 NPs, we also performed FTIR analysis (Fig. 3). The data revealed the presence of vibrational peaks that belong to organic functional groups, indicating the presence of GER. In particular, the broadband in the range of 3.500–3.000 cm^{-1} was observed in the anatase and rutile TiO_2 NPs, which is related to the stretching of hydroxyl groups (O–H), indicating the presence of surface water as moisture (Fig. 3A and B). The FTIR spectrum of anatase TiO_2 NPs (Fig. 3A) showed a typical band on 1630 cm^{-1} that is attributed to the H–O–H vibrations from physisorbed water [19, 20] and an absorption band detected at 438 cm^{-1} that belongs to the Ti–O–Ti vibrations related to the anatase phase [21, 22]. Similar absorption band peaks were observed in the case of rutile TiO_2 NPs (Fig. 3B), with the exception of the Ti–O–Ti vibration, which is shifted and detected at 512 cm^{-1} as a result of the temperature increase (900 °C) during rutile preparation [18, 21]. Investigating the molecular vibration features of the GER-modified TiO_2 NPs, we detected additional peaks indicating successful surface modification. In the case of anatase TiO_2 NPs (Fig. 3A), the vibrational peaks detected at 3406 cm^{-1} and 1639 cm^{-1} are related to the O–H groups coming from surface and physisorbed water, similar to the case of unmodified TiO_2 NPs. The peaks detected at 2970 cm^{-1}, 2922 cm^{-1}, and 2871 cm^{-1} belong to the CH stretching vibrations of GER [19, 23], while the stretching vibrations at 1710 cm^{-1}, corresponding to the carbonyl group (C=O), confirm the consumption of hydroxyl groups from GER during surface modification of TiO_2 [24, 25]. The stretching of other peaks at 493 cm^{-1} and 573 cm^{-1} belongs to TiO_2 [18]. A similar position of detected peaks can be observed in the case of rutile TiO_2 NPs modified with GER (Fig. 3B). The only exception is the deformed C–H bending vibrations detected in two peaks at 1377 cm^{-1} and 1439 cm^{-1}, which belong to the methylene ($–CH_2–$) and methyl ($–CH_3$) groups [24], confirming the interaction of GER with TiO_2 NPs.

In addition to the analyses described above, the FTIR spectra of free GER and GER-modified TiO_2 NPs were examined, and the results showed notable alterations in peak locations indicating GER-TiO_2 interaction (Figure S1). For instance, in the rutile and anatase GER-modified TiO_2 NPs, the O-H stretching vibration peak

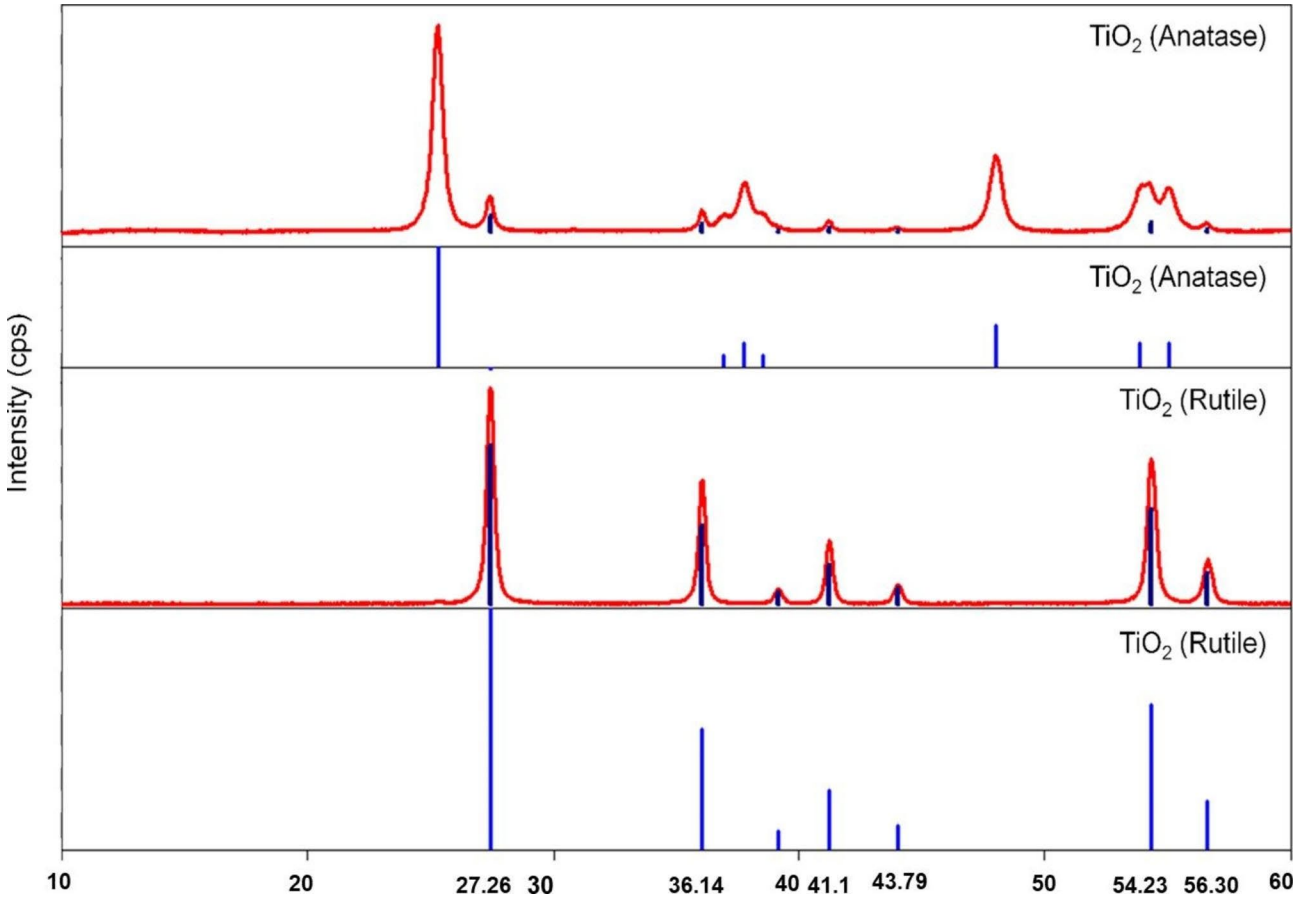

Fig. 2 X-ray powder diffraction patterns of anatase and rutile form of TiO_2.

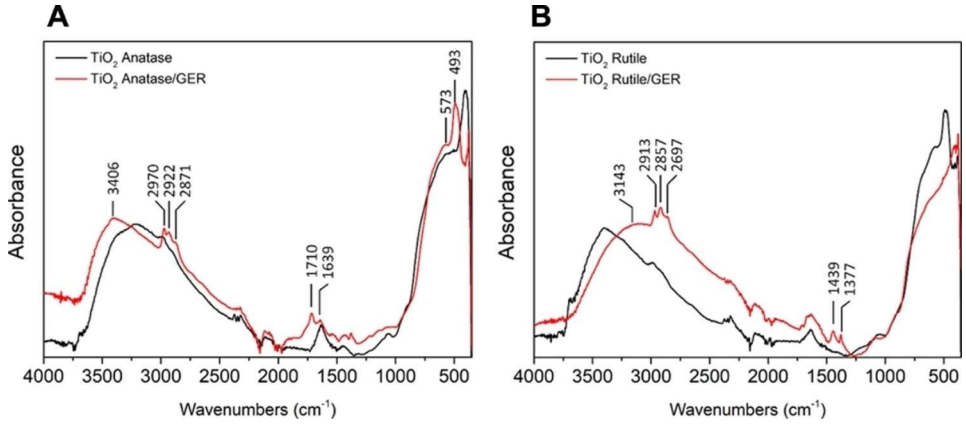

Fig. 3 Baseline-corrected FTIR spectra of the TiO_2/anatase and TiO_2/anatase/geraniol (**A**) and TiO_2/rutile and TiO_2/rutile/geraniol (**B**) in the 4000 to 400 cm^{-1} range

changed from 3.330 cm^{-1} in free GER to 3.406 cm^{-1} and 3.143 cm^{-1}, respectively. Similar considerable changes in the C-H bending and stretching vibrations of the -CH_2 and -CH_3 groups were seen after surface modification. These peak shifts show the impact of GER-TiO_2 interactions on the vibrational behavior of these functional groups and confirm the effective surface modification of TiO_2 NPs with GER. Additional characteristics of our synthesized TiO_2 nanoparticles, including particle size distribution and zeta potential, are further explored in the supplementary materials (Figure S2 and S3).

Table 1 Minimum inhibitory concentration (MIC) and FIC index of GER, anatase, and rutile and their combination against various bacterial strains

Bacteria	Component	MIC (mg/ml)	FIC Index	Description
MRSA	Anatase	2	NaN	Indifference
MRSA	Rutile	2	NaN	Indifference
MRSA	GER	4.25	NaN	Indifference
MRSA	Anatase/GER	1	0.735294	Additive
MRSA	Rutile/GER	1	0.735294	Additive
S. aureus	Anatase	1.5	NaN	Indifference
S. aureus	Rutile	1.5	NaN	Indifference
S. aureus	GER	2.125	NaN	Indifference
S. aureus	Anatase/GER	0.25	0.284314	Synergism
S. aureus	Rutile/GER	0.25	0.284314	Synergism
E. coli	Anatase	1.5	NaN	Indifference
E. coli	Rutile	1.5	NaN	Indifference
E. coli	GER	4.25	NaN	Indifference
E. coli	Anatase/GER	0.25	0.22549	Synergism
E. coli	Rutile/GER	0.25	0.22549	Synergism

* Note: "NaN" in the FIC index column indicates that the Fractional Inhibitory Concentration (FIC) was not calculated for the respective component against the particular bacterial strain

Effect of TiO_2/GER treatments on bacteria

It was observed that both TiO_2/anatase/GER and TiO_2/rutile/GER exhibit activity against *S. aureus*, MRSA, and *E. coli*, with MIC values ranging from 0.25 to 1.0 mg/ml (Table 1). In contrast, anatase and rutile forms alone did not display any strong bactericidal properties, and GER displayed indifferent activity with MIC values of 4.25 mg/ml The interaction between GER and TiO_2 inhibitory was confirmed by the FIC index values, which showed additive effects in the case of MRSA with a value of 0.735294 and synergism for *S. aureus* and *E. coli* with values of 0.284314 and 0.22549 respectively (Table 1). Furthermore, the supporting data can be found in (Figure S4, and Tables S1 and S2). Live and dead assays showed that the viability of *S. aureus*, MRSA, and *E. coli* was significantly reduced after treatment with both TiO_2/anatase/GER and TiO_2/rutile/GER. At concentrations of 0.25 mg/ml and 0.5 mg/ml, dead cells (stained in red) and live cells (stained in green) were barely visible, indicating that the treatment had a bactericidal effect on all strains, including the MRSA (Fig. 4). Images of control samples showed an increase of live cells (stained in green) and a decrease in dead cells (stained in red).

Biofilm assay

It was observed that TiO_2/anatase/GER treatment was highly effective against the MRSA biofilm, reducing its growth by 84.6% ($p<0.0001$). Similarly, the TiO_2/rutile/GER treatment reduced the biofilm growth by 80% ($p<0.0001$). We also measured the effect of UV light (c 280 nm) under the same conditions and found that after 60 min, the results were similar to the non-UV light treatment, with the exception of a significant reduction in viability after geraniol treatment compared to that of the negative control (bacteria alone) (Fig. 5A and B).

Confocal laser microscopy was employed for a more qualitative, in-depth evaluation of the mixed TiO_2 nanoparticles (NPs) with GER on MRSA biofilm. By analyzing fluorescence intensity distribution, it was found that both TiO_2/anatase/GER and TiO_2/rutile/GER significantly reduced biofilm thickness to values less than 30,000 nm compared to that of the control ($p<0.0001$) (Fig. 6A). Interestingly, the treatment with anatase and

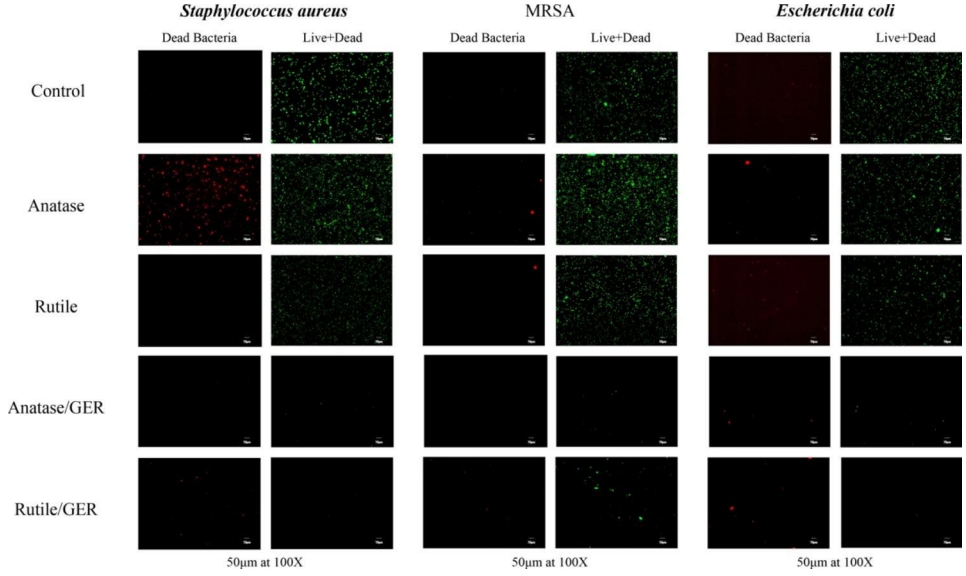

Fig. 4 The LIVE/DEAD cell images of *S. aureus*, MRSA, and *E. coli* treated with TiO_2 anatase, TiO_2 rutile, TiO_2 /anatase/GER, and TiO_2 /rutile/GER—magnification 100×. The scale bar is 50 µm. The saturation was processed equally across all micrographs

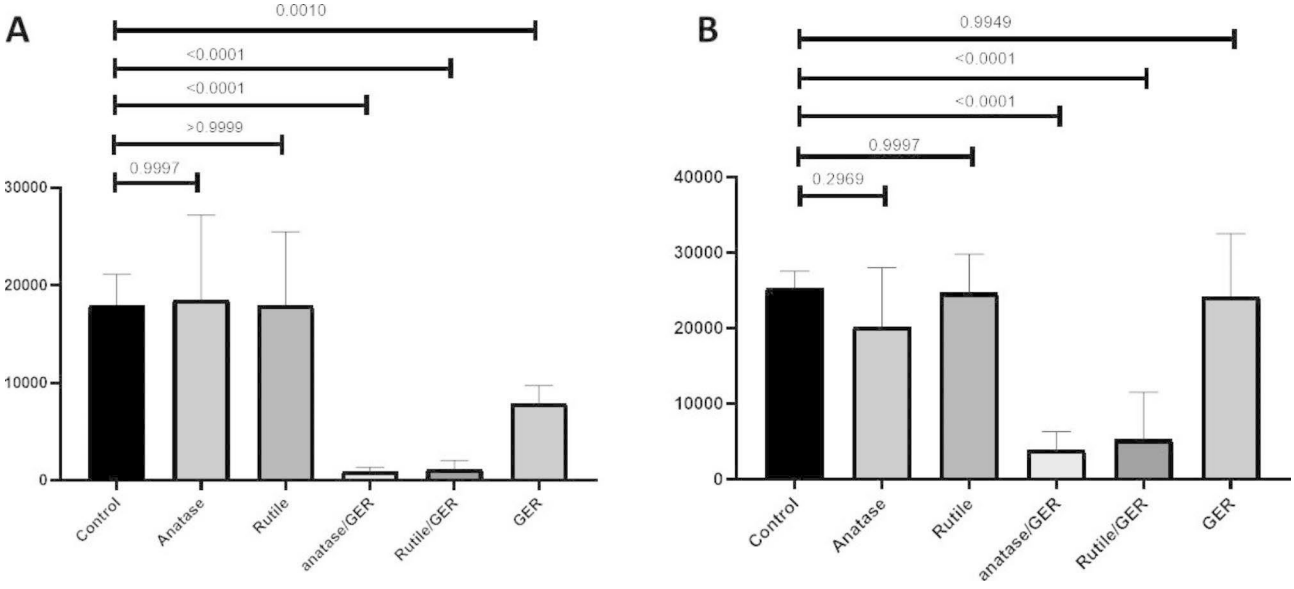

Fig. 5 Fluorescence intensity (a.u.) of bacterial biofilm: Efficiency of modified and non-modified TiO_2 against MRSA biofilm with UV-irradiation **A**) and without UV irradiation **B**).

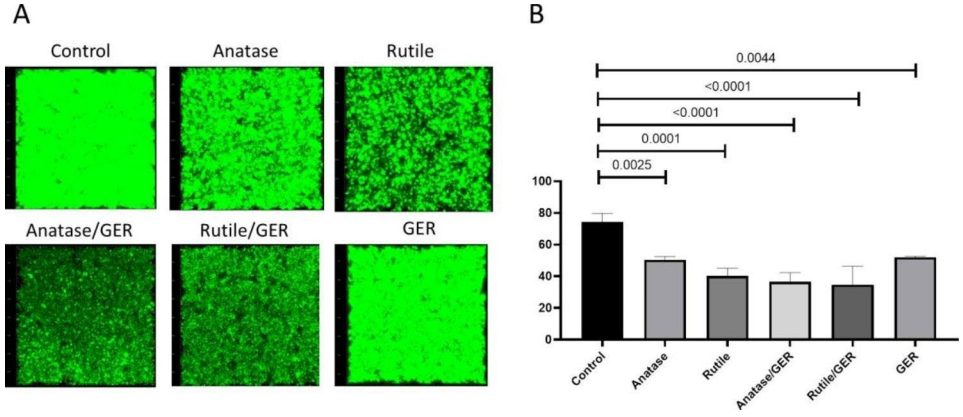

Fig. 6 **A)** 3D images from confocal laser scanning microscopy of cells in biofilm with intact membranes (green) and disturbed bacterial biofilm (black areas). **B**) Biofilm thickness after different treatments.

rutile forms alone also decreased the biofilm thickness (Fig. 6B).

Discussion

Titanium dioxide NPs have the potential to function as antimicrobial agents with several chemical modifications to optimize their biochemical properties. In this work, we report the synthesis and characterization of TiO_2 NPs in anatase and rutile forms together with surface modification by GER for antibacterial effect enhancement. The antibacterial and antifungal properties of TiO_2 against a broad range of pathogens were demonstrated in several previous studies [21] and the use of natural compounds to enhance physical and chemical properties of NPs has also been documented [30, 31, 39]. In our study, GER was chosen as a potential candidate for coupling with TiO_2 to enhance its antimicrobial properties due to its high solubility and controlled toxicity [40, 41].

The morphology of the TiO_2 NPs can be tuned by calcination temperature [44]. In line with previous reports [45–47], we successfully synthesized TiO_2 with two different calcination temperatures, 500 °C confirming the creation of TiO_2 in the anatase form and 900 °C to generate TiO_2 in the rutile form. The success of TiO_2/GER modification was confirmed by the XRD results showing the impact of homogenization on the crystalline structure of the combination [48, 49]. Another verification of the successful modification was done by elemental composition with EDS. Carbon was a definite indicator of response and coverage in the sample. Several earlier studies have detected the presence of carbon, which is

attributed to carbon-containing functional groups of natural products [50–52].

Several investigations employing modification of TiO_2 demonstrated the antibacterial activity of this material [53]. These studies attributed the increase in antimicrobial susceptibility to modifications of TiO_2 with natural elements and non-metallic compounds [45, 46, 54, 55]. Our MIC results are consistent with previous findings reporting MIC against various G-positive and G-negative bacteria in the similar range [45, 56–59] while other studies reported the MIC against MRSA to be much higher (7.0–13.0 mg/ml) [60, 61]. Our study showed that the UV light on TiO_2 had no significant changes in the reduction rate. This finding contradicts a previous report that suggested that UV light irradiation of TiO_2 nanorod arrays exhibited excellent antibacterial properties against both *S. aureus* and *E. coli* biofilm [40].

Although the confocal microscopy results supported the quantitative Alamar blue results, some variation was noticed. In the Alamar blue analysis, both TiO_2 modifications exhibited greater effectiveness against MRSA biofilms, and neither treatment alone had a statistically significant effect on the biofilms. In contrast, the confocal microscopy indicated that the different TiO_2 treatments influenced the architecture of the biofilms, as they showed a reduction in biofilm thickness. These findings are supported by previous studies emphasizing the importance of examining biofilms using quantitative and qualitative methods [45]. Therefore, we have demonstrated that TiO_2 has the potential to act as an anti-biofilm agent on its own without the need for any modification.

The increased antimicrobial activity and reduction in bacterial cell viability due to the exposure of TiO_2/anatase/GER and TiO_2/rutile/GER showed that both treatments had a high adsorption capacity on the cell surface. The increased antimicrobial activity of modified TiO_2 can be explained by several mechanisms. First, geraniol ability to adhere to cell membrane lipids of bacteria can mediate antimicrobial activity by increasing the permeabilization of the membrane [62, 63]. In addition, the presence of TiO_2, TiO_2/anatase/GER, and TiO_2/rutile/GER can lead to loss of cell wall integrity and direct interaction with DNA leading to cell death [64, 65]. Secondly, modifications of NPs are commonly used to prevent aggregation, allowing them to disperse in aqueous environments or other hydrophilic media, thereby enhancing their antimicrobial activity [47]. Lastly, modifications are also one of the most effective methods to regulate and control NPs and bacteria interactions and increase ROS production [31, 32].

Based on these findings, combining TiO_2 with geraniol, offers an opportunity for the antibacterial use. Low cytotoxic effects, described in Figure S5., highlight the usefulness of these compounds. Nevertheless, further research is needed to find out the full range of potential applications and any additional potential hazards.

Conclusions

In conclusion, TiO_2 nanoparticles modified with GER in the form of anatase and rutile were successfully synthesized and tested for their antimicrobial activity. The modified TiO_2 nanoparticles had the elevated antimicrobial activity and also inhibited MRSA biofilm formation. TiO_2 alone also proved to be effective against biofilms.

Methods

Preparation of TiO_2 NPs

Titanium isopropoxide (1.48 ml) (Sigma Aldrich in St. Louis, MO, USA) was mixed with 229.0 µl of isopropyl alcohol (Lach-Ner in Neratovice, Czech Republic) and 18.0 µl of MilliQ water (pH 8) (Thermofisher, USA) and stirred for 10 min. Then, the solution was washed three times with MilliQ water and dried overnight in the Memmert UM 400 drying oven (Memmert, Schwabach, Germany) at 60 °C. Finally, TiO_2 NPs were produced by calcining the dried solution at the temperature of 500 °C for the anatase form and 900 °C for the rutile form for 2 h in the laboratory chamber furnace (LAC in Rajhrad, Czech Republic).

Modification of TiO_2 NPs by GER

The TiO_2 NPs were redispersed in 50 ml of MilliQ water. Then, 10 ml of the dispersion with 161.1 mg of GER (Sigma Aldrich, Saint Louis, USA) was mixed in 200 µl of GER solvent with MilliQ water and stirred overnight. Afterward, the solution was washed three times with MilliQ water.

Characterization of TiO_2 NPs

The absorbance wavelength was determined using the UV/Vis spectrophotometer (Perkin-Elmer, USA) with the quartz cuvette with acetonitrile/tetrahydrofuran as a reference. The X-ray powder diffraction patterns of the TiO_2 NPs were recorded on the Bruker 8D advanced X-ray diffractometer (Bruker, AXS GmbH, Karlsruhe, Germany) with CuKα radiation of wavelength = 1.54056 Å. The morphology of the TiO_2 NPs was studied by SEM using the JEOL JSM-6330 LA operated at 20.0 kV and 1.0000 nA. The elemental analysis used SEM on a Tescan MIRA 2 equipped with a FEG (Tescan Ltd., Brno, Czech Republic) and EDX detector MAX 50 (Oxford Instruments plc, Abingdon, UK). The images were obtained using the E-T SE detector at a working distance of 15 mm and 15 kV acceleration voltages, with 50 000-fold magnification. Fourier transform infrared spectroscopy (FTIR) analysis was used on a film of each freeze-dried sample using a Jasco FT/IR-4700 (Jasco, MD, USA) spectrophotometer with a wavenumber range of 400 to 4000 cm^{-1} with 4 cm^{-1} resolutions. The zeta potential and size of particles were measured using the dynamic light scattering technique on the Zeta sizer Nano ZS instrument (Malvern Instrument

Ltd, UK). The particle size distribution and ζ-potential were studied using dynamic light scattering (DLS) on the Malvern Zetasizer (NANO-ZS, Malvern Instruments Ltd., Worcestershire, U.K.) at a detector angle of 173° and the refractive index of 1.33 at 25 °C. The size distribution and ζ-potential measurements were performed in MilliQ water at pH 6.8. Measurements were taken for each sample in triplicates.

Determination of minimum inhibitory concentration (MIC)

Bacterial cultures were obtained from the Czech Collection of Microorganisms (Brno, Czech Republic), including *Staphylococcus aureus* CCM 4223, MRSA CCM 7110, and *Escherichia coli* CCM 3954. All bacterial strains were cultured on Columbia agar with 5% sheep blood (LMS, Czech Republic) at 37 °C for 24 h. The antibacterial activity of TiO_2/anatase/GER, TiO_2/rutile/GER, along with control treatments anatase, rutile, and GER, was evaluated against bacterial strains cultured in Muller Hinton broth (company). Bacteria were incubated in the 96 well plate at 37 °C, with 150 rpm shaking; the optical density (OD) at 600 nm was measured after 24 h.

Determination of fractional inhibitory concentration (FIC)

The effect of the GER and TiO_2 combination was assessed against bacterial strains using the checkerboard technique [16]. We then calculated the FIC index values using the formula: FICI=FIC (A)+FIC (B). The Σ FICI values were interpreted as follows:

≤0.5=synergistic; >0.5–1.0=additive; > 1.0–4.0=indifferent (non-interactive); > 4.0=antagonistic.

LIVE/DEAD® Cell Assay

Live/dead assay was carried out by following the manufacturer instructions of the LIVE/DEAD™ BacLight™ bacterial viability kit for microscopy (Invitrogen, USA). Modified nanomaterials TiO_2/anatase/GER, TiO_2/rutile/GER, and non-modified anatase and rutile samples were examined at the defined MIC after 24 h and these bacterial samples were observed by an inverted fluorescent microscope Olympus IX71 (Olympus C&S Ltd., Czech Republic).

MRSA biofilm assay

The efficacy of TiO_2 with and without GER agent. MRSA biofilm was evaluated using qualitative and quantitative methods. MRSA was incubated in BHI with 1% glucose for 72 h at 37 °C. Biofilms were treated based on the MIC values, washed twice with PBS, and stained with the alamarBlue™ cell viability reagent (Invitrogen, USA) for 20 min. The 96 well plate was used to carry out the experiment, and biofilm viability was measured using fluorescence measurements (Tecan, Switzerland) (590/570 nm, excitation/emission). Qualitative assessment of the biofilm thicknesses and high-quality visualization images were done using confocal microscopy (LSM 880, USA) with the incubation and washing conditions, with the exception that IBIDI dishes were used and stained using the LIVE/DEAD™ BacLight™ bacterial viability kit for microscopy (Invitrogen, USA).

Abbreviations

NPs	Nanoparticles
GER	Geraniol
SEM	Scanning electron microscopy
EDS	Electron-dispersive spectroscopy
FTIR	Fourier transform infrared spectroscopy
DLS	Dynamic light scattering
MIC	Minimum inhibitory concentration
FIC	Fractional inhibitory concentration
OD	Optical density
MRSA	Methicillin-resistant *Staphylococcus aureus*
BHI	Brain heart infusion
PBS	Phosphate-buffered saline

Supplementary Information

The online version contains supplementary material available at https://doi.org/10.1186/s12866-023-02955-1.

Supplementary Material 1

Acknowledgements

Not Applicable.

Authors' contributions

ABY performed experiments, analyzed and commented on microbiological parts, and completed and wrote the article. TF performed a microscopy measurement. KS helped in the editing and arrangement of data. HM performed a cytotoxicity experiment. PS performed SEM and EDX analyses. PA performed FTIR analysis. PK and VM designed and supervised the analysis and data evaluation of XRD, SEM, EDX, FTIR. VA supervised the project. LZ supervised the writing of the article. KD designed the experiment, supervising and approving the microbiological data.

Funding

Funding was supported by the ERDF "Multidisciplinary research to increase application potential of nanomaterials in agricultural practice" (No. CZ.02.1.01/0.0/0.0/16_025/0007314) and by the Internal Grant Agency of Mendel University in Brno (AF-IGA2020-IP068).

Data Availability

Data is available on the department share drive and can be uploaded by the first author when requested.

Declarations

Ethics approval and consent to participate

Not applicable.

Consent for publication

Not applicable.

Competing interests

The authors declare that they have no competing interests.

Received: 1 March 2023 / Accepted: 21 July 2023
Published online: 02 August 2023

References

1. Murray CJ, Ikuta KS, Sharara F, Swetschinski L, Aguilar GR, Gray A, et al. Global burden of bacterial antimicrobial resistance in 2019: a systematic analysis. The Lancet. 2022;399(10325):629–55.

2. Coyle JR, Freeland M, Eckel ST, Hart AL. Trends in morbidity, mortality, and cost of hospitalizations associated with infectious disease sequelae of the opioid epidemic. J Infect Dis. 2020;222(Supplement5):451–S7.
3. Li H, He J, Liang J, Liang Y, Zheng W, Qu Q et al. Opposing implications of co-evolutionary lineages and traits of gut microbiome on human health status. bioRxiv. 2023:2023.05. 30.542569.
4. Ansarian Barezi A, Shakerian A, Rahimi E, Esfandiari Z. Examining the Extent of Contamination, Antibiotic Resistance, and Genetic Diversity of Clostridioides (Clostridium) difficile Strains in Meat and Feces of Some Native Birds of Iran. BioMed Research International. 2023;2023.
5. Suprenant MP, Ching C, Sutradhar I, Gross N, Anderson JE, El Sherif N et al. Impact of Zinc Pre-exposure on de novo Antibiotic Resistance Development. bioRxiv. 2023:2023.04. 10.536219.
6. Yuan H, Ma Q, Ye L, Piao G. The traditional medicine and modern medicine from natural products. Molecules. 2016;21(5):559.
7. Basavegowda N, Baek K-H. Multimetallic nanoparticles as alternative Antimicrobial Agents: Challenges and Perspectives. Molecules. 2021;26(4):912.
8. Gold K, Slay B, Knackstedt M, Gaharwar AK. Antimicrobial activity of metal and metal-oxide based nanoparticles. Adv Ther. 2018;1(3):1700033.
9. Celardo I, Pedersen JZ, Traversa E, Ghibelli L. Pharmacological potential of cerium oxide nanoparticles. Nanoscale. 2011;3(4):1411–20.
10. Arreche R, Bellotti N, Blanco M, Vázquez P. Synthesis and characterization of zirconium oxides for use as antimicrobial additives in paints. Procedia Mater Sci. 2015;9:627–34.
11. Nguyen N-YT, Grelling N, Wetteland CL, Rosario R, Liu H. Antimicrobial activities and mechanisms of magnesium oxide nanoparticles (nMgO) against pathogenic bacteria, yeasts, and biofilms. Sci Rep. 2018;8(1):16260.
12. Liu K, Cheng F, Luo Y, Liu L, Wang C, Xie K, et al. Porous single crystalline-like titanium dioxide monolith with enhanced photoelectrochemical performance. Front Mater. 2023;10:1177093.
13. Alshibeh Alwattar N, Vacandio F, Vassalo L, Djenizian T, Coulomb B, Boudenne J-L, editors. Effects of Mode of Preparation of Titanium Dioxide Nanotube arrays on their Photocatalytic Properties: application to p-Nitroaniline degradation. Micro: MDPI; 2023.
14. Lowry GV, Gregory KB, Apte SC, Lead JR. Transformations of nanomaterials in the environment. ACS Publications; 2012.
15. Oktar N, Yetmez F, Ficai M, Ficai D, Dumitru A, Pica F. Molecular mechanism and targets of the antimicrobial activity of metal nanoparticles. Curr Top Med Chem. 2015;15(16):1583–8.
16. Ibáñez JA, Litter MI, Pizarro RA. Photocatalytic bactericidal effect of TiO2 on Enterobacter cloacae: comparative study with other Gram (–) bacteria. J Photochem Photobiol A. 2003;157(1):81–5.
17. Wyszogrodzka G, Marszałek B, Gil B, Dorożyński P. Metal-organic frameworks: mechanisms of antibacterial action and potential applications. Drug Discovery Today. 2016;21(6):1009–18.
18. Abdal Dayem A, Hossain MK, Lee SB, Kim K, Saha SK, Yang G-M, et al. The role of reactive oxygen species (ROS) in the biological activities of metallic nanoparticles. Int J Mol Sci. 2017;18(1):120.
19. Sandulescu A, Anastasescu C, Papa F, Raciulete M, Vasile A, Spataru T, et al. Advancements on Basic Working Principles of Photo-Driven oxidative degradation of Organic Substrates over Pristine and Noble Metal-Modified TiO2. Model case of Phenol Photo Oxidation. Catalysts. 2021;11(4):487.
20. Reddy PVL, Kavitha B, Reddy PAK, Kim K-H. TiO2-based photocatalytic disinfection of microbes in aqueous media: a review. Environ Res. 2017;154:296–303.
21. Anandgaonker P, Kulkarni G, Gaikwad S, Rajbhoj A. Synthesis of TiO2 nanoparticles by electrochemical method and their antibacterial application. Arab J Chem. 2019;12(8):1815–22.
22. Allen NS, Mahdjoub N, Vishnyakov V, Kelly PJ, Kriek RJ. The effect of crystalline phase (anatase, brookite and rutile) and size on the photocatalytic activity of calcined polymorphic titanium dioxide (TiO2). Polym Degrad Stab. 2018;150:31–6.
23. Polli AD, Lange FF, Levi CG. Metastability of the fluorite, pyrochlore, and perovskite structures in the PbO—ZrO2—TiO2 system. J Am Ceram Soc. 2000;83(4):873–81.
24. Foster HA, Ditta IB, Varghese S, Steele A. Photocatalytic disinfection using titanium dioxide: spectrum and mechanism of antimicrobial activity. Appl Microbiol Biotechnol. 2011;90:1847–68.
25. Vimbela GV, Ngo SM, Fraze C, Yang L, Stout DA. Antibacterial properties and toxicity from metallic nanomaterials. Int J Nanomed. 2017;12:3941.
26. Scarpelli F, Mastropietro TF, Poerio T, Godbert N. Mesoporous TiO2 thin films: state of the art. Titanium Dioxide-Material for a Sustainable Environment. 2018;508(1):135–42.
27. Braydich-Stolle LK, Schaeublin NM, Murdock RC, Jiang J, Biswas P, Schlager JJ, et al. Crystal structure mediates mode of cell death in TiO2 nanotoxicity. J Nanopart Res. 2009;11(6):1361–74.
28. Lu Z-X, Zhou L, Zhang Z-L, Shi W-L, Xie Z-X, Xie H-Y, et al. Cell damage Induced by Photocatalysis of TiO2 Thin Films. Langmuir. 2003;19(21):8765–8.
29. Li K, Qian J, Wang P, Wang C, Fan X, Lu B, et al. Toxicity of three crystalline TiO2 nanoparticles in activated sludge: bacterial cell death modes differentially weaken sludge dewaterability. Environ Sci Technol. 2019;53(8):4542–55.
30. Kashyap D, Tuli HS, Yerer MB, Sharma A, Sak K, Srivastava S, et al. editors. Natural product-based nanoformulations for cancer therapy: Opportunities and challenges. Seminars in cancer biology. Elsevier; 2021.
31. Badeggi UM, Ismail E, Adeloye AO, Botha S, Badmus JA, Marnewick JL, et al. Green synthesis of gold nanoparticles capped with procyanidins from Leucosidea sericea as potential antidiabetic and antioxidant agents. Biomolecules. 2020;10(3):452.
32. du Maire P, Deckert M, Johlitz M, Öchsner A. Characterisation of the mechanical properties of polyamide 12 powder when using titanium dioxide as antimicrobial additive. Materialwiss Werkstofftech. 2023;54(4):385–90.
33. Kassalia M-E, Chorianopoulos N, Nychas G-J, Pavlatou EA. Investigation of the Photoinduced Antimicrobial Properties of N-Doped TiO2 nanoparticles under visible-light irradiation on Salmonella Typhimurium Biofilm. Appl Sci. 2023;13(7):4498.
34. Cha BJ, Saqlain S, Seo HO, Kim YD. Hydrophilic surface modification of TiO2 to produce a highly sustainable photocatalyst for outdoor air purification. Appl Surf Sci. 2019;479:31–8.
35. Bui VKH, Park D, Lee Y-C. Chitosan Combined with ZnO, TiO2 and ag nanoparticles for Antimicrobial Wound Healing applications: a Mini Review of the Research Trends. Polymers. 2017;9(1):21.
36. Zhao Y, Wang Y, Xiao G, Su H. Fabrication of biomaterial/TiO2 composite photocatalysts for the selective removal of trace environmental pollutants. Chin J Chem Eng. 2019;27(6):1416–28.
37. Kusworo TD, Ariyanti N, Utomo DP. Effect of nano-TiO2 loading in polysulfone membranes on the removal of pollutant following natural-rubber wastewater treatment. J Water Process Eng. 2020;35:101190.
38. Zhang J, Liu Q, He H, Shi F, Huang G, Xing B, et al. Coal tar pitch as natural carbon quantum dots decorated on TiO2 for visible light photodegradation of rhodamine B. Carbon. 2019;152:284–94.
39. Jadhav R, Pawar P, Choudhari V, Topare N, Raut-Jadhav S, Bokil S et al. An overview of antimicrobial nanoparticles for food preservation. Materials Today: Proceedings. 2022.
40. Regev S, Cone WW. Analyses of pharate female twospotted spider mites for nerolidol and geraniol: evaluation for sex attraction of males. Environ Entomol. 1976;5(1):133–8.
41. Chen W, Viljoen AM. Geraniol — a review of a commercially important fragrance material. South Afr J Bot. 2010;76(4):643–51.
42. Mayabadi AH, Waman VS, Kamble MM, Ghosh SS, Gabhale BB, Rondiya SR, et al. Evolution of structural and optical properties of rutile TiO2 thin films synthesized at room temperature by chemical bath deposition method. J Phys Chem Solids. 2014;75(2):182–7.
43. Maheswari P, Ponnusamy S, Harish S, Muthamizhchelvan C, Ganesh MR, Hayakawa Y. Hydrothermal syntheses and characterization of bio-modified TiO2 nanoparticles with Aqua Rosa and protein powder for their biological applications. Appl Surf Sci. 2019;494:989–99.
44. Hameed RS, Fayyad RJ, Nuaman RS, Hamdan NT, Maliki SAJ. Synthesis and characterization of a Novel Titanium Nanoparticals using Banana Peel Extract and investigate its Antibacterial and Insecticidal Activity. J Pure Appl Microbiol. 2019;13(4):2241–9.
45. Abu-Dalo M, Jaradat A, Albiss BA, Al-Rawashdeh NAF. Green synthesis of TiO2 NPs/pristine pomegranate peel extract nanocomposite and its antimicrobial activity for water disinfection. J Environ Chem Eng. 2019;7(5):13.
46. Ahmadi R, Tanomand A, Kazeminava F, Kamounah FS, Ayaseh A, Ganbarov K, et al. Fabrication and characterization of a titanium dioxide (TiO2) nanoparticles reinforced bio-nanocomposite containing Miswak (Salvadora persica L.) extract - the antimicrobial, thermo-physical and barrier properties. Int J Nanomed. 2019;14:3439–54.
47. Bahmani M, Taherikalani M, Khaksarian M, Rafieian-Kopaei M, Ashrafi B, Nazer M, et al. Synthesis and evaluation of the Antibacterial Effect of Titanium Dioxide Nanoparticles in comparison with Ampicillin, Colistin, and Ertapenem on Staphylococcus aureus. J Pharm Negat Results. 2019;10(1):16–20.

48. Lu P-J, Huang S-C, Chen Y-P, Chiueh L-C, Shih DY-C. Analysis of titanium dioxide and zinc oxide nanoparticles in cosmetics. J food drug Anal. 2015;23(3):587–94.
49. Zhang Q, Fan W, Gao L. Anatase TiO2 nanoparticles immobilized on ZnO tetrapods as a highly efficient and easily recyclable photocatalyst. Appl Catal B. 2007;76(1–2):168–73.
50. Saiful Amran SNB, Wongso V, Abdul Halim NS, Husni MK, Sambudi NS, Wirzal MDH. Immobilized carbon-doped TiO2 in polyamide fibers for the degradation of methylene blue. J Asian Ceam Soc. 2019;7(3):321–30.
51. Rosliza R, Izman S. SEM-EDS characterization of natural products on corrosion inhibition of Al-Mg-Si alloy. Prot Met Phys Chem Surf. 2011;47(3):395–401.
52. Tisserand R, Young R. 2 - Essential oil composition. In: Tisserand R, Young R, editors. Essential Oil Safety (Second Edition). St. Louis: Churchill Livingstone; 2014. p. 5–22.
53. Younis AB, Haddad Y, Kosaristanova L, Smerkova K. Titanium dioxide nanoparticles: recent progress in antimicrobial applications. Wiley Interdisciplinary Reviews: Nanomedicine and Nanobiotechnology. 2022:e1860.
54. Arezoo E, Mohammadreza E, Maryam M, Abdorreza MN. The synergistic effects of cinnamon essential oil and nano TiO2 on antimicrobial and functional properties of sago starch films. Int J Biol Macromol. 2020;157:743–51.
55. Zhang T, Li ZQ, Wang WB, Wang Y, Gao BY, Wang ZN. Enhanced antifouling and antimicrobial thin film nanocomposite membranes with incorporation of Palygorskite/titanium dioxide hybrid material. J Colloid Interface Sci. 2019;537:1–10.
56. Azizi-Lalabadi M, Ehsani A, Divband B, Alizadeh-Sani M. Antimicrobial activity of Titanium dioxide and zinc oxide nanoparticles supported in 4A zeolite and evaluation the morphological characteristic. Sci Rep. 2019;9:10.
57. Deshmukh SP, Mullani SB, Koli VB, Patil SM, Kasabe PJ, Dandge PB, et al. Ag nanoparticles connected to the surface of TiO2 electrostatically for antibacterial photoinactivation studies. Photochem Photobiol. 2018;94(6):1249–62.
58. Desai V, Kowshik M. Synthesis and characterization of fumaric acid functionalized AgCl/titania nanocomposite with enhanced antibacterial activity. J Nanosci Nanotechnol. 2013;13(4):2826–34.
59. Chegeni M, Pour SK, Dizaji BF. Synthesis and characterization of novel antibacterial Sol-gel derived TiO2/Zn2TiO4/Ag nanocomposite as an active agent in Sunscreens. Ceram Int. 2019;45(18):24413–8.
60. Ansari MA, Albetran HM, Alheshibri MH, Timoumi A, Algarou NA, Akhtar S, et al. Synthesis of electrospun TiO2 nanofibers and characterization of their antibacterial and antibiofilm potential against gram-positive and gram-negative bacteria. Antibiotics. 2020;9(9):572.
61. Senarathna U, Fernando S, Gunasekara T, Weerasekera M, Hewageegana H, Arachchi N, et al. Enhanced antibacterial activity of TiO2 nanoparticle surface modified with Garcinia zeylanica extract. Chem Cent J. 2017;11(1):1–8.
62. Basavegowda N, Baek K-H. Combination strategies of different antimicrobials: an efficient and alternative Tool for Pathogen inactivation. Biomedicines. 2022;10(9):2219.
63. Swamy MK, Akhtar MS, Sinniah UR. Antimicrobial properties of plant essential oils against human pathogens and their mode of action: an updated review. Evidence-Based Complementary and alternative medicine. 2016;2016.
64. Kubacka A, Diez MS, Rojo D, Bargiela R, Ciordia S, Zapico I, et al. Understanding the antimicrobial mechanism of TiO2-based nanocomposite films in a pathogenic bacterium. Sci Rep. 2014;4(1):1–9.
65. Xiang Y, Ran Q, Wu C, Zhou L, Zhang W, Li J, et al. Single-cell transcriptomics uncovers the impacts of titanium dioxide nanoparticles on human bone marrow stromal cells. Chem Eng J. 2022;440:135814.

Publisher's Note